



## PAPER

## Measurements of dipole moments and a Q-patch model of collisionally charged grains

## OPEN ACCESS

RECEIVED  
18 May 2020REVISED  
24 July 2020ACCEPTED FOR PUBLICATION  
11 August 2020PUBLISHED  
10 September 2020

Original content from  
this work may be used  
under the terms of the  
[Creative Commons  
Attribution 4.0 licence](#).

Any further distribution  
of this work must  
maintain attribution to  
the author(s) and the  
title of the work, journal  
citation and DOI.

Tobias Steinpilz , Felix Jungmann , Kolja Joeris , Jens Teiser  and  
Gerhard Wurm 

Faculty of Physics, University of Duisburg-Essen, Lotharstr. 1-21, 47057 Duisburg, Germany

E-mail: [tobias.steinpilz@uni-due.de](mailto:tobias.steinpilz@uni-due.de)**Keywords:** electrical dipole moment, static charge, triboelectric effect, experimental measurements, computer simulation, Q-patch modelSupplementary material for this article is available [online](#)**Abstract**

Identical glass spheres of  $434 \pm 17 \mu\text{m}$  diameter are charged in collisions among each other. At slow speed some form dimers under microgravity and oscillate within the electrical field of a capacitor. The dipole moments deduced from these oscillations are large. They cannot be explained by the net charges measured for each grain (up to  $\pm 3 \times 10^5 e$ ) and show no significant dependence on the net charge in the given range. This requires a highly non-homogeneous charge distribution on the grain surface. We simulate heterogeneous charging with a Q-patch charging model in agreement to the experimental data.

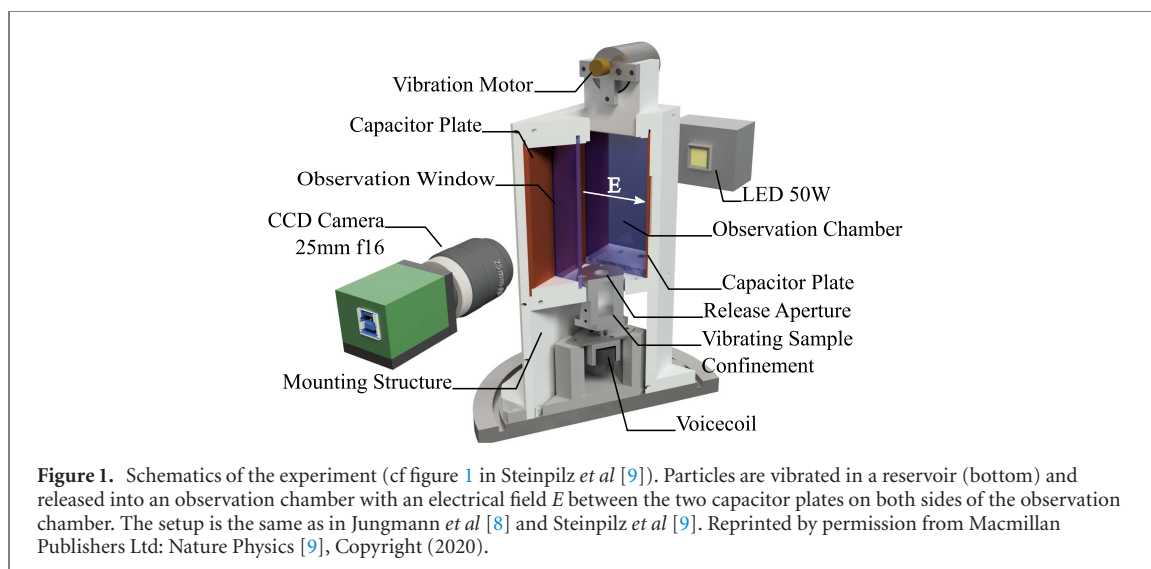
**1. Introduction**

It is known for centuries that charge is transferred between two different materials on contact [1–4]. If the material is the same but grain sizes or contact radii are different, there is also charge separation [5, 6]. However, even if grains are of the same material and have the same size, i.e. if grains are as identical as they can be, charge is still exchanged [7–9].

This charging is important in the context of aggregation. Lee *et al* [10] observed charged grains in Kepler like orbits and also find small symmetric aggregates with differently charged grains in microgravity experiments. Steinpilz *et al* [9] just found that grains can aggregate to cm size in the context of planet formation if they are charged.

Due to the asymmetry of collisions, insulating grains might not charge homogeneously [11]. This is especially true for identical colliding grains since both signs of charge might be transferred randomly and grains that carry no net charge, can nevertheless have a surface with complex charge distribution. Along this line, Jungmann *et al* [8] could only explain the sticking behavior of grains colliding with an electrode if they assumed an offset charge which requires an inhomogeneous charge distribution on the surface. Recently Grosjean *et al* [12] treated inhomogeneously charged surfaces in great detail. Also, Steinpilz *et al* [9] observed aggregates, where all constituent grains have the same sign of charge but stick together. This requires higher order contributions to the electric field, which might be induced dipoles [13] or permanent but inhomogeneously distributed charges. It is currently unclear how the charge distribution on the surface of collisionally charged grains looks like.

In a microgravity experiment we studied collisionally charged grains in a homogeneous field of a plate capacitor. This allows a measurement of the net charge on each grain. At the same time, we found a number of cases where two grains of known charge collide within the capacitor and merge into a dimer. This dimer then oscillates within the electrical field of the capacitor. Using the oscillation frequency, the known electrical field strength and the particle properties, it is possible to calculate the electrical dipole moment of the dimer.



Naively, one might expect the dipole moment to originate from the two net charges placed somewhere on the spheres. However, even under the assumption of extreme distances between charges, we could not explain the oscillations (see below) and also induced dipoles could not be held responsible. Therefore, this experiment offers the rare opportunity to get a glimpse on the heterogeneity of the surface charges mentioned above and we compare our dipole measurements to the results of a numerical Q-patch model which charges grains heterogeneously in collisions.

## 2. Experiments

The experiment was carried out under microgravity in the drop tower Bremen. Launching the experiment by a catapult provides about 9 s of microgravity time with residual accelerations negligible for this study. The experiment is sketched in figure 1.

An experimental run has the following sequence: a sample of identical ( $434 \pm 17 \mu\text{m}$  diameter, for a size distribution see Steinpilz *et al* [9]) soda lime glass spheres with around 0.9 mass percentage water (measured with a scale by heating to  $160^\circ\text{C}$ ) is placed inside the vibrating sample confinement. The whole setup is then evacuated to around  $5 \times 10^{-2}$  mbar and afterwards flushed with  $\text{CO}_2$  to 1 bar two times to ensure a reproducible atmosphere with 0% relative humidity. As described by e.g. Shahraeni and Or [14] it is possible to calculate the water content of a porous sample at atmospheric pressure in case the temperature and the relative humidity of the environment are known. The precise starting water content after the flushing procedure of our sample is unknown. In addition the other components e.g. vacuum chamber or the observation chamber are not negligible as they also participate to the relative humidity in our setup. Therefore the calculation is beyond the scope of this paper as it would be based on multiple estimations. We can only conclude the upper limit for the sample water content with  $0.9 \pm 0.2\%$ . While the experiment is still on the ground the confinement is vibrated for 15 min with around 35 Hz. The experiment is then launched. During microgravity the grains leave the confinement through a small opening in the top. This happens either due to relaxation of the setup after the acceleration or by stronger vibration of the sample confinement. The grains then enter a capacitor with an electrical field up to  $83 \text{ kV m}^{-1}$ . Charged grains follow parabolic trajectories due to their net charge which are shown in figure 2. The given resolution of our optical system is  $13 \text{ pixel mm}^{-1}$  and the frame rate 180 fps.

Figure 2 actually shows an example of two grains on intersecting trajectories, colliding and sticking to each other, forming a dimer. It is curious that the grains stick together though they do have the same sign charge (in this example) and sticking occurs against Coulomb repulsion. However, sticking in these cases is likely promoted by attractive forces of dipoles induced in the dielectric grains. For two charged grains Qin *et al* [15] found that same sign charges still allow for attractive forces if the charge ratio is within a certain range. Around 25% of our charge pairs have ratios of 3 or more which would fit in this scheme. In addition, dipoles induced by the external field of the capacitor, although not being responsible for the oscillations (see below), also provide attractive forces.

In any case, this dimer is then oscillating, visualized by a number of lines in figure 2 indicating the symmetry axis of the dimer (two additional examples can be found as supplementary videos ([stacks.iop.org/NJP/22/093025/mmedia](https://stacks.iop.org/NJP/22/093025/mmedia))). Analysis of the oscillation allows to determine the dipole moment and the charge distribution on the dimer, in addition to the net charge of the two individual grains.

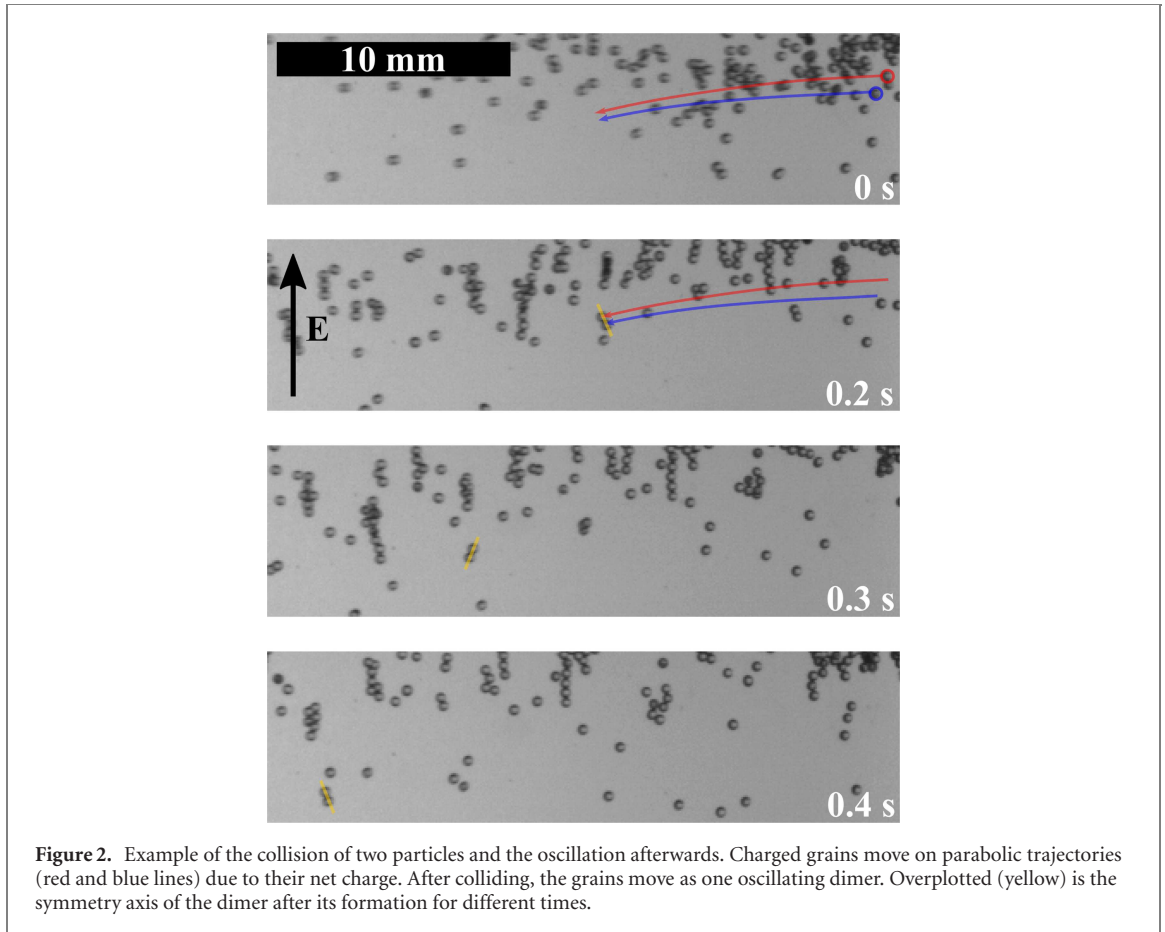


**Figure 2.** Example of the collision of two particles and the oscillation afterwards. Charged grains move on parabolic trajectories (red and blue lines) due to their net charge. After colliding, the grains move as one oscillating dimer. Overplotted (yellow) is the symmetry axis of the dimer after its formation for different times.

Stokes gas drag due to the ambient  $\text{CO}_2$  atmosphere corresponds to a force of around  $6 \times 10^{-10}$  N for a relatively fast particle with  $2 \text{ cm s}^{-1}$ . This is approximately 60% of the electrical force, due to the capacitor, for an averagely charged particle with  $1.3 \times 10^{-14}$  C. The gas drag only alters the measured net charges within the shown error bars. Compared to the motion of the center of mass, the oscillation velocity is much slower and gas drag only dampens the oscillation marginally on the observed timescales (approx. 2 s unobstructed movement). Therefore we neglect the gas drag for the measurement of the oscillation frequency.

### 3. Oscillations of dipoles

The observed oscillations are one dimensional around an axis perpendicular to the electrical field and through the center of mass—see black dot in figure 3. Due to the symmetry of the dimer consisting of identical grains, the center of mass is the contact point of the grains. The line of sight of the camera coincides with a projection of the rotation axis and the projection of the rotation angle  $\alpha$  can be measured from 2D images.

The oscillation can be described by the equation of motion

$$M = J \frac{d\alpha}{dt} \quad (1)$$

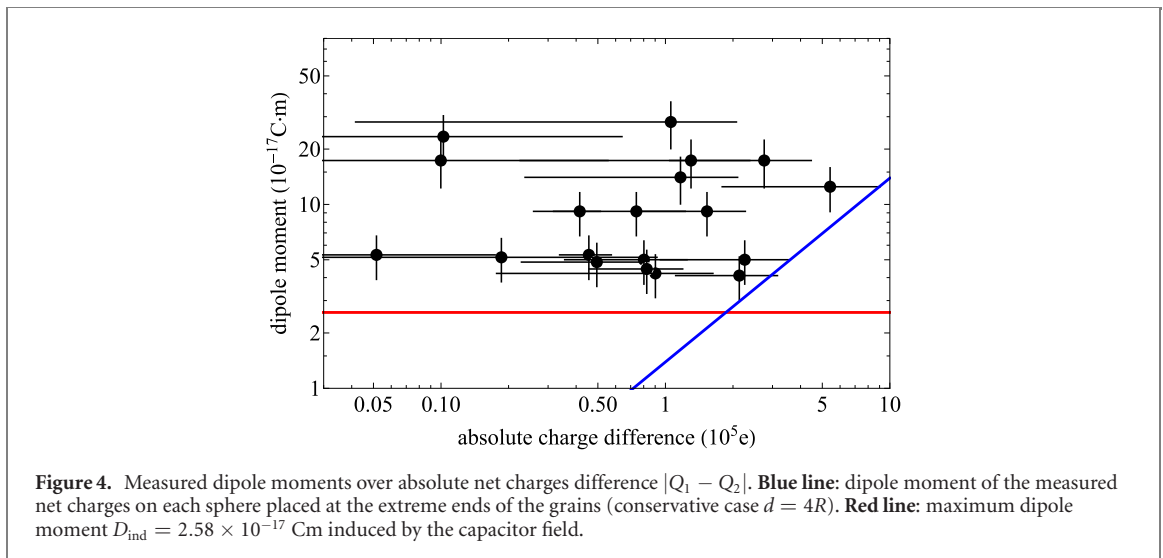
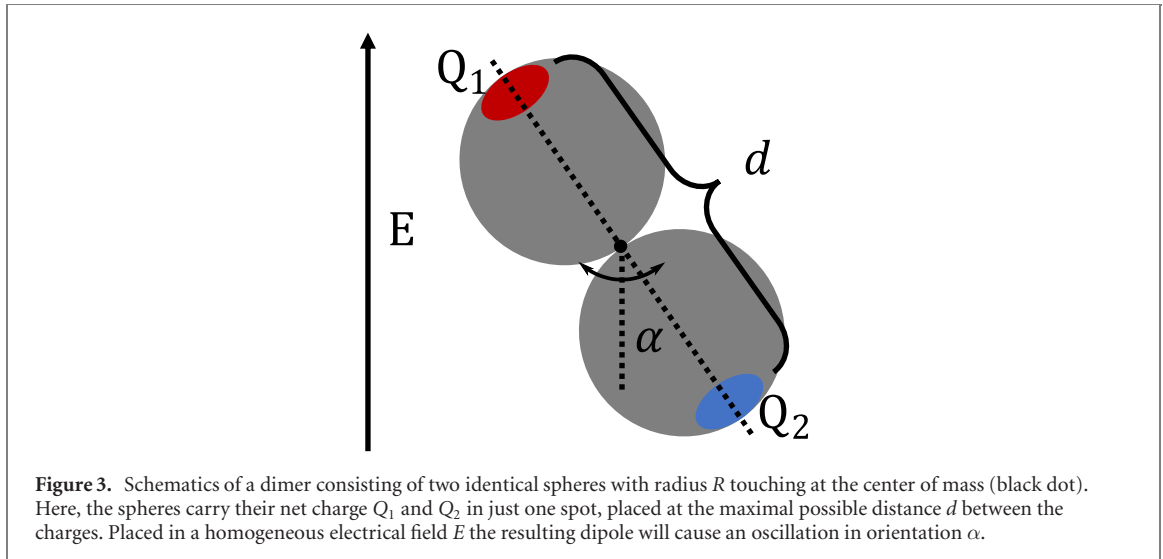
where,  $M$  is the torque and  $J$  is the moment of inertia around the rotation axis. The torque is given as

$$M = ED \sin \alpha \quad (2)$$

with the electrical field  $E$  and the dipole moment  $D$ , defined as the sum of all  $N$  (discrete) charges  $Q_i$  times the distances  $R_i$  from the contact point or

$$D = \left| \sum_{i=1}^N Q_i \vec{R}_i \right|. \quad (3)$$

The moment of inertia for the two spheres of radius  $R$  and mass  $m$  is  $14/5 \cdot m \cdot R^2$  (homogeneous spheres and Steiner's parallel-axis theorem). Solving equations (1) and (2) for a harmonic oscillation leads



to the frequency  $\omega$

$$\omega = \sqrt{\frac{E}{J} D}. \quad (4)$$

Using the values of  $\omega$  measured from the observed oscillations, it is possible to calculate the electrical dipole moments  $D$  which cause these oscillations,

$$D = \frac{14\pi}{5E} m R^2 \omega^2. \quad (5)$$

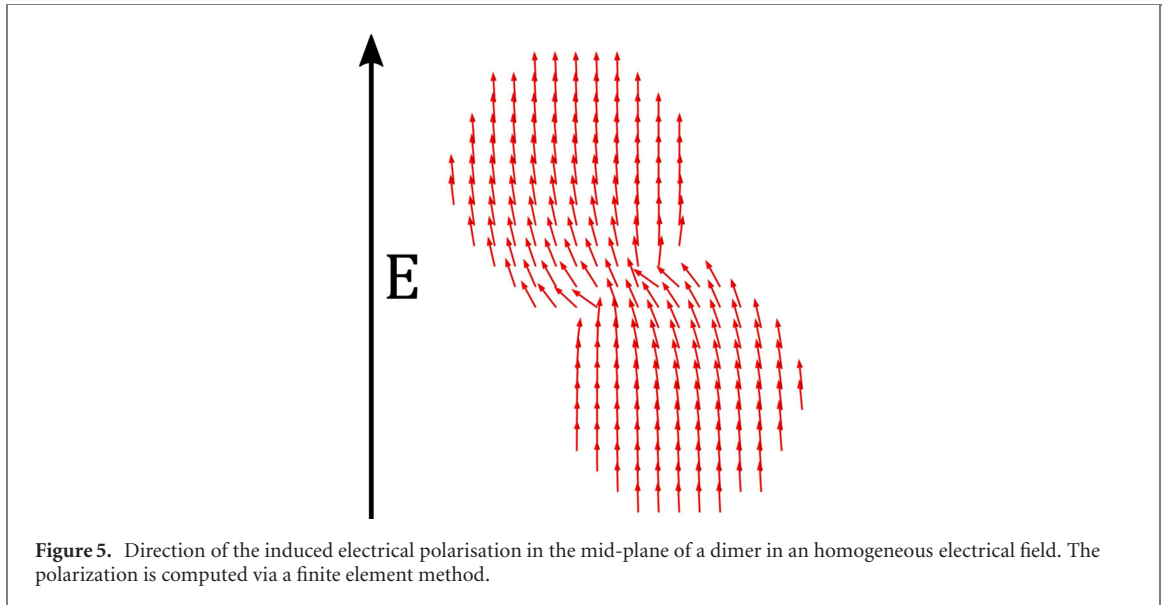
Here, the mass  $m$  of a single sphere is  $m = 111 \pm 16 \mu\text{g}$ . The radius  $R$  of a sphere is  $R = 217 \pm 8 \mu\text{m}$ . An electrical field of  $E = 42$  or  $83 \text{ kV m}^{-1}$  was applied.

These measured dipole moments are shown in figure 4. There seems to be no significant dependency on the absolute net charge difference between the two single spheres.

#### 4. Dipole models and charge configurations

For two dielectric spheres, three dipole models are reasonable to explain these measurements:

- simple dipole due to the two net charges.
- induced dipoles due to the external electrical field.
- complex charge distributions on the surface.



#### 4.1. Net charge dipole

This is the most simple charge configuration to be considered and usually the one that comes to mind first—a simple schematic view is shown in figure 3. Within the dimers studied, grains tend to have opposite net charges, a positive  $Q_{1+}$  and a negative  $Q_{2-}$ . These net charges might be placed on the grains in different ways. As is often considered, it might be distributed homogeneously or, equivalently, placed in the center of the grains. In this case the dipole moment is

$$D_{\text{net}} = QR \quad (6)$$

with  $Q = Q_{1+} - Q_{2-}$ .

However, Jungmann *et al* [8] showed that the center of charge might not be the center of the sphere. The most conservative estimate here (largest dipole moment) would assume that both charges are placed exactly at the opposite ends of the dimer. In this case, the maximum dipole moment would be twice as high as for the homogeneous distribution or

$$D_{\text{netmax}} = 2QR. \quad (7)$$

Anyway, in both cases the measured dipole should linearly increase with the charge difference  $Q$ . The most conservative case is shown in figure 4 as blue line. This is far below the measured dipole moments. Especially, the dipoles of the dimers having a small absolute charge difference cannot be explained by this simple model. Thus, net charges cannot be considered as origin of the dipole moments we measured.

#### 4.2. Induced dipole

Next, we estimate the dipole moments that are induced in the dielectric dimer by the external electrical field of the capacitor. In principle, these induced dipoles can be very large.

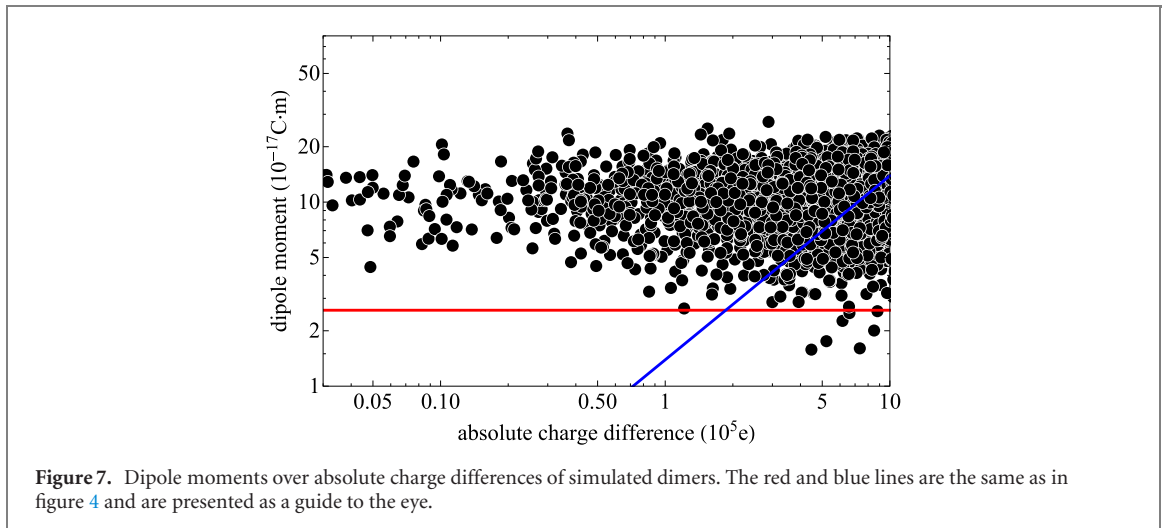
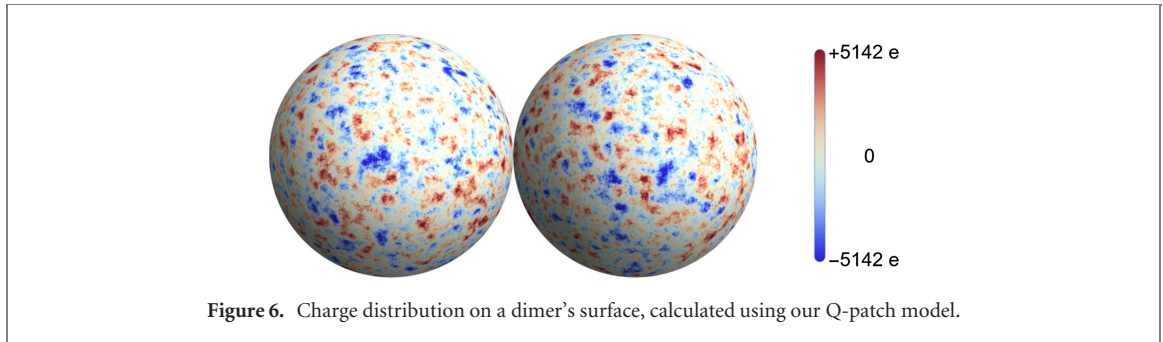
For simple cases it can be calculated analytically, such as the dipole moment of a single dielectric sphere in an electrical field [16]:

$$D_{\text{ind}} = 4\pi\epsilon_0 \frac{\epsilon_r - 1}{\epsilon_r + 2} R^3 E. \quad (8)$$

The permittivity of soda lime glass is about  $\epsilon_r = 7.3$  [17]. For an electrical field  $E = 83 \text{ kV m}^{-1}$  this leads to the induced dipole moment of a single sphere  $D_{\text{ind}} = 6.4 \times 10^{-17} \text{ Cm}$ , which is within the range of the measured dipole moments.

However, in a symmetric configuration, this does not induce any additional torques as it always points along the electrical field, whatever its strength. Only in the case of a non-symmetric particle shape, there are dipole components perpendicular to the electrical field which then result in a torque. During oscillation in an external electric field a dimer breaks the symmetry so that a dipole moment and torque occur. The polarisation induced in a dimer is visualized in figure 5 for an rotational angle of  $\alpha = 30^\circ$ .

The induced polarisation which contributes a torque is calculated using the finite element method provided by COMSOL 4.3. To verify the results we first simulated a single sphere in an electrical field. The numerical calculation matches the analytic result given in equation (8). Simulating the dipole moments of a



dimer for different angles  $\alpha$  shows that the dipole moment responsible for the torque follows a harmonic

$$D(\alpha) = D_{\text{ind}} \sin 2\alpha, \quad (9)$$

having a maximum at  $45^\circ$  and being zero at  $90^\circ$ . This factor 2 in equation (9) can be understood as at  $90^\circ$  the geometry is symmetric again and torques vanish. Beyond  $90^\circ$  the torque changes sign and would accelerate the dimer the other way round.

In any case, the most conservatively simulated maximal dipole moment is  $D_{\text{ind}} = 2.58 \times 10^{-17}$  Cm. This is plotted as red line in figure 4 and is well below the measured values. Therefore, also the induced dipoles cannot account for the measured dipole moments.

#### 4.3. Q-patch model

As these two simple models cannot explain the oscillations, the charge distribution on the surface of the grains has to generate a permanent dipole moment not related to any net charge. Especially, if one considers that the charges on the grain's surface are transferred during collisions, it is likely that the surface is composed of many patches of different charges, providing a dipole moment. As a first approach we compare our results with a simple Q-patch model, where charges are transferred according to some rules each time two grains get in contact. This is similar to the 2D model of [18] but more extended.

In this model, charges are located on the grain's surface. Each grain surface consists of 100 000 points, distributed on a sphere using the Fibonacci lattice by Gonzalez [19]. Each point carries a charge, initialized to be zero.

The collisions are performed in the form of a list operation. For each point on the sphere there exists a list of its neighbors, ordered by proximity. At each collision  $i$ , a charge  $q_i$ , a central point  $p_i$  and a patch size radius  $s_i$ , are chosen. The charge  $q_i$  is then added to each of the points around  $p_i$ , which lie within the patch size  $s_i$ . To determine  $s_i$ , an integer is drawn from the interval [5, 100]. The patch then consists of the neighbors in the range of  $s_i$  around  $p_i$ . This corresponds to a patch radius of  $3.3\text{--}12.9 \mu\text{m}$  for our  $434 \mu\text{m}$  sized grains. The charge  $q_i$  is drawn from an exponential distribution with a damping factor of one, analog to the distribution used by Haerberle *et al* [20] and found in our experiments in Steinpilz *et al* [9]. Afterwards, the charge sign is chosen randomly.

This procedure is repeated for 75 individual spheres for 150 000 collisions each, while the charge configuration is saved after every 10 000 collisions. To increase the sample size, 1500 combinations of two spheres are drawn, which have at least undergone 30 000 collisions. Figure 6 shows an example of the charge distribution on a dimer. For those drawn dimers the charge difference of the grains and the maximum combined dipole moment are calculated. We do not know exactly, how much charge is transferred in each collision in our experiment. So we use this uncertainty by scaling the resulting charge of the simulation by a factor of 70 to reach net charge values which are comparable to the measurements. The simulation's scaled results are shown in figure 7. Scaling the charge does not change the geometry of the system. This means, the point cloud in the figure can only be shifted diagonally—we can not obtain arbitrary combinations of charges and dipoles.

As expected, our model does not perfectly replicate the measurements. Anyway, using a reasonable scaling factor, which yields to a reasonable charge transfers per collision of 3600  $e$  on average and 70 000  $e$  at max, the simulated grain's properties are similar to the experimental ones and give an idea what surface charge distribution can be expected. This might be measurable by Kelvin probe microscopy, as done by e.g. Baytekin *et al* [21].

## 5. Conclusion

For small grains it is often not feasible to determine charge distributions on the surface and net charges are taken as approximation for all charge related processes. However, we show here the presence of significant dipole moments which are not necessarily correlated to the net charges. Even essentially uncharged grains can have large dipole moments. This can be explained by patches of charge on the grain's surface and has significant consequences.

Jungmann *et al* [8] showed that the sticking velocity, the speed below which two grains stick after a collision, strongly depends on the charge. To explain that behavior a model based on the net charge but displaced from the center has been used. In view of our results this might rather be the effect of the multipole surface. Also net neutral grains with multipole charge distribution might stick at much higher velocities than grains without significant net charge.

With respect to sticking, Steinpilz *et al* [9] found stable aggregates composed of grains where each grain was of the same sign of charge. It is possible that one highly charged grain can induce dipoles in the others and promote sticking [13, 22]. Also grains of same sign charge can stick this way [15]. However, Coulomb repulsion should destroy these aggregates in most cases if only net charges were present. Here, complex charge patterns as found in this paper easily promote sticking and can explain the observed same sign of charge clusters.

## Acknowledgments

Our thanks go to Lea Spieker for her work on tracing particles. This project is supported by DLR Space Administration with funds provided by the Federal Ministry for Economic Affairs and Energy (BMWi) under Grant numbers DLR 50 WM 1762 and DLR 50 WM 1943. We acknowledge support by the Open Access Publication Fund of the University of Duisburg-Essen.

## ORCID iDs

Tobias Steinpilz  <https://orcid.org/0000-0001-5375-2618>

Felix Jungmann  <https://orcid.org/0000-0002-0269-2763>

Kolja Joeris  <https://orcid.org/0000-0002-5841-2636>

Jens Teiser  <https://orcid.org/0000-0003-4468-4937>

Gerhard Wurm  <https://orcid.org/0000-0002-7962-4961>

## References

- [1] Feng J Q 2000 *Phys. Rev. E* **62** 2891
- [2] Lacks D J and Sankaran R M 2011 *J. Phys. D Appl. Phys.* **44** 453001
- [3] Siu T, Cotton J, Mattson G and Shinbrot T 2014 *Phys. Rev. E* **89** 052208
- [4] Méndez Harper J and Dufek J 2016 *J. Geophys. Res.: Atmos.* **121** 8209
- [5] Waitukaitis S R, Lee V, Pierson J M, Forman S L and Jaeger H M 2014 *Phys. Rev. Lett.* **112** 218001
- [6] Lee V, James N M, Waitukaitis S R and Jaeger H M 2018 *Phys. Rev. Mater.* **2** 035602

- [7] Yoshimatsu R, Araújo N A M, Wurm G, Herrmann H J and Shinbrot T 2017 *Sci. Rep.* **7** 39996
- [8] Jungmann F, Steinpilz T, Teiser J and Wurm G 2018 *J. Phys. Commun.* **2** 095009
- [9] Steinpilz T, Joeris K, Jungmann F, Wolf D, Brendel L, Teiser J, Shinbrot T and Wurm G 2020 *Nat. Phys.* **16** 225
- [10] Lee V, Waitukaitis S R, Miskin M Z and Jaeger H M 2015 *Nat. Phys.* **11** 733
- [11] Yoshimatsu R, Araújo N A M, Shinbrot T and Herrmann H J 2016 *Soft Matter* **12** 6261
- [12] Grosjean G, Wald S, Sobarzo J C and Waitukaitis S 2020 arXiv:2006.07120v5
- [13] Matias A F V, Shinbrot T and Araújo N A M 2018 *Phys. Rev. E* **98** 062903
- [14] Shahraeeni E and Or D 2010 *Langmuir* **26** 13924
- [15] Qin J, Li J, Lee V, Jaeger H, de Pablo J J and Freed K F 2016 *J. Colloid Interface Sci.* **469** 237
- [16] Jones T B 1995 *Electromechanics of Particles* (Cambridge: Cambridge University Press)
- [17] Ashby M F 2013 *Materials and the Environment* 2nd edn (Oxford: Butterworth-Heinemann) pp 459–595
- [18] Jungmann F, Steinpilz T, Teiser J and Wurm G 2018 *69th International Astronautical Congress (Bremen)*
- [19] Gonzalez A 2010 *Math. Geosci.* **42** 49
- [20] Haerberle J, Schella A, Sperl M, Schröter M and Born P 2018 *Soft Matter* **14** 4987
- [21] Baytekin H T, Patashinski A Z, Branicki M, Baytekin B, Soh S and Grzybowski B A 2011 *Science* **333** 308
- [22] Siu T, Pittman W, Cotton J and Shinbrot T 2015 *Granular Matter* **17** 165

# DuEPublico

Duisburg-Essen Publications online

UNIVERSITÄT  
DUISBURG  
ESSEN

*Offen im Denken*

ub | universitäts  
bibliothek

This text is made available via DuEPublico, the institutional repository of the University of Duisburg-Essen. This version may eventually differ from another version distributed by a commercial publisher.

**DOI:** 10.1088/1367-2630/abae43  
**URN:** urn:nbn:de:hbz:464-20210119-171809-0



This work may be used under a Creative Commons Attribution 4.0 License (CC BY 4.0) .